X-ray Structures and Emissive and Second-Order Nonlinear Optical Properties of Two Inorganic−Organic Polymeric Adducts of CuI with 4-Acetylpyridine. The Role of Both "Intrastrand" Charge Transfers and Structural Motifs on the Nonlinear Optical Response of Cu(I) Polymeric Adducts with Pseudoaromatic η^1-Nitrogen Donor Ligands

Elena Cariati,*[,†] Dominique Roberto,[†] Renato Ugo,[†] Peter C. Ford,[‡] Simona Galli,*[,§] and Angelo Sironi[||]

Dipartimento di Chimica Inorganica, Metallorganica e Analitica, and Dipartimento di Chimica Strutturale e Stereochimica Inorganica, Università degli Studi di Milano, and Istituto di Scienze e Tecnologie Molecolari del CNR (ISTM-CNR), Via Venezian 21, I-20133 Milano, Italy, Department of Chemistry, University of California, Santa Barbara, California, 93106, and Dipartimento di Scienze Chimiche, Fisiche e Matematiche, Università dell'Insubria, Via Valleggio 11, I-22100 Como, Italy

Received June 27, 2002. Revised Manuscript Received October 2, 2002

X-ray crystal structures, solid-state photoluminescence, and Kurtz−Perry powder second harmonic generation (SHG) efficiencies of two novel noncentrosymmetric polymeric adducts of CuI with 4-acetylpyridine, a double-stranded "stair" and a single-stranded "chain", are reported, the latter being a rare example of a $[CuX(L)_2]_n$ motif (X = halide, L = pseudoaromatic η^1-nitrogen donor ligand). In a series of structurally related noncentrosymmetric $[CuX(L)]_n$ chains and stairs, the powder SHG responses are interpreted in terms of both structural motifs (chains showing definitely greater efficiency than stairs) and "intrastrand" charge transfers involving the bridging halides.

Introduction

Recently, the investigation for new materials exhibiting worth emissive and nonlinear optical (NLO) properties has been focused on inorganic−organic compounds, which can properly mingle the advantages of both the inorganic species (higher chemical, thermal, and mechanical stabilities) and the organic ones (appreciable response speed and intensity in a wide spectral range, straightforward synthetic approach).[1] Moreover, extremely important synergistic effects such as electron-transfer processes between the inorganic and the organic counterparts may introduce additional optical,[2] magnetic,[3] or electric[4] properties.

Among the inorganic−organic materials, the adducts between copper(I) halides (CuX, with X = Cl, Br, or I) and pseudoaromatic ligands bearing an η^1-nitrogen donor atom (L) are potentially promising, for both the variety of structural motifs displayed and the peculiar emissive properties.[5,6] Actually, structural motifs such as $[CuX(L)]$ monomers,[7] $[CuX(L)_2]_2$ dimers,[8] $[CuX(L)]_4$ tetramers,[9] and $[CuX(L)]_n$ single-stranded "zig-zag chain"[10] and double-stranded "stair"[11] polymers have been reported. Photoluminescence properties have been systematically analyzed only for CuI tetramers:[6,12] their solid-state, room-temperature low-energy (LE) yellow emission (centered around 580−625 nm) has been interpreted as a decay from a triplet "cluster centered"

* Corresponding author. Phone: (+39)-0250314460. Fax: (+39)-0250314454. E-mail: simona@csmtbo.mi.cnr.it.

† Dipartimento di Chimica Inorganica, Metallorganica e Analitica, Università degli Studi di Milano, and Istituto di Scienze e Tecnologie Molecolari del CNR (ISTM-CNR).

‡ University of California.

§ Università dell'Insubria.

|| Dipartimento di Chimica Strutturale e Stereochimica Inorganica, Università degli Studi di Milano, and Istituto di Scienze e Tecnologie Molecolari del CNR (ISTM-CNR).

(1) Consult, for example: (a) Nalwa, H. S. *Appl. Organomet. Chem.* **1991**, *5*, 349 and references therein. (b) Long, N. J. *Angew. Chem., Int. Ed. Engl.* **1995**, *34*, 21 and references therein.

(2) See, for example: (a) Coradin, T.; Clèment, R.; Lacroix, P. G.; Nakatani, K. *Chem. Mater.* **1996**, *8*, 2153. (b) Guloy, A. M.; Tang, Z.; Miranda, P. B.; Srdanov, V. I. *Adv. Mater.* **2001**, *13*, 833.

(3) Consult, for example: (a) Lacroix, P. G.; Clèment, R.; Nakatani, K.; Zyss, J.; Ledoux, I. *Science* **1994**, *263*, 658. (b) Bénard, S.; Yu, P.; Audière, J. P.; Rivière, E.; Clèment, R.; Guilhem, J.; Tchertanov, L.; Nakatani, K. *J. Am. Chem. Soc.* **2000**, *122*, 9444. (c) Lacroix, P. G.; Malfant, I.; Bénard, S.; Yu, P.; Rivière, E.; Nakatani, K. Chem. Mater. **2001**, *13*, 441.

(4) See, for example: Andreu, R.; Malfant, I.; Lacroix, P. G.; Gornitzka, H.; Nakatani, K. *Chem. Mater.* **1999**, *11*, 840.

(5) (a) Masse, R. *J. Opt. Soc. Am. B* **1992**, *9*, 534. (b) Henary, M.; Wootton, J. L.; Khan, S. I.; Zink, J. I. *Inorg. Chem.* **1997**, *36*, 796. (c) Kotler, Z.; Hierle, R.; Josse, D.; Zyss, J.; Khodja, S.; Josse, D.; Zyss, J. *J. Opt. Soc. Am. B* **1998**, *15*, 751.

(6) Ford, P. C.; Cariati, E.; Bourassa, J. *Chem. Rev.* **1999**, *99*, 3625 and references therein.

(7) The reader is referred to, for example: (a) Healy, P. C.; Pakawatchai, C.; White, A. H. *J. Chem. Soc., Dalton Trans.* **1983**, 1917. (b) Dyason, J. C.; Healy, P. C.; Pakawatchai, C.; Patrick, V. A.; White, A. H. *Inorg. Chem.* **1985**, *24*, 1957. (c) Dyason, J. C.; Engelhardt, L. M.; Healy, P. C.; Kildea, J. C.; White, A. H. *Aust. J. Chem.* **1988**, *41*, 335. (d) Jedrzejas, M. J.; Martuch, R. A.; Towns, R. L. R.; Baker, R. J.; Duraj, S. A.; Hepp, S. F. *Acta Crystallogr. Sect. C* **1993**, *49*, 536.

10.1021/cm020640w CCC: $22.00
Published on Web 11/12/2002

(^{3}CC*) excited state (ES). The latter involves the I_4 and Cu_4 tetrahedra and has mixed halide-to-metal charge-transfer (^{3}XMCT*) and $d_{Cu} \rightarrow (s,p)_{Cu}$ character. Copper···copper distances lower than the sum of the van der Waals radii (2.80 Å) have been invariably found and considered as an indirect proof of the $d_{Cu} \rightarrow (s,p)_{Cu}$ contribution, for which a significant overlap among the orbitals of the Cu_4 core is required.[6,12] At variance, the solid-state room-temperature emissive behavior of polymers has been investigated just for a few double-stranded stairs (namely, $[CuI(pyridine)]_n$ (**1**),[6] $[CuI(3\text{-methylpyridine})]_n$ (**2**),[13] and $[CuI(4\text{-methylpyridine})]_n$ (**3**)[13]). For the high-energy (HE) blue emissions observed (respectively centered at 437, 454, and 437 nm), a decay from a triplet halide-to-ligand charge transfer (^{3}XLCT*) ES has been invoked. Any contribution from metal-delocalized orbitals has been discarded on the basis of intermetal distances greater than 2.80 Å.

Despite the evidence of significant charge-transfer processes, no systematic investigations have been performed on the solid-state second-order NLO responses of oligomeric and polymeric CuX/L adducts. Here we report the syntheses, the crystal structures, and the emissive and solid-state second-order NLO properties of two noncentrosymmetric chain and stair polymeric adducts between CuI and 4-acetylpyridine (**4a**, **4b**). To highlight both the electronic processes and the structural aspects that may govern their second-order NLO response, we examined both the solid-state second harmonic generation (SHG) and the emissive behavior of some structurally related noncentrosymmetric $[CuX(L)]_n$ chains and stairs, namely, $[CuCl(quinoline)]_n$ (**5**),[11h] $[CuCl(2\text{-methylquinoline})]_n$ (**6**),[10c] $[CuBr(pyridine)]_n$ (**7**),[11e,14] $[CuBr(2,4,6\text{-trimethylpyridine})]_n$ (**8**),[10c] $[CuBr(2\text{-methylquinoline})]_n$ (**9**),[10c] and $[CuI(2,4,6\text{-trimethylpyridine})]_n$ (**10**).[10c] This body of information allowed an attempted individuation of both the intrastrand charge-transfer (CT) processes and the structural features controlling SHG in these polymeric materials.

Experimental Section

Synthesis and Characterization of Compounds 4−10. Synthesis of $[CuI(4\text{-acetylpyridine})]_n$ (4a). Compound **4a** was prepared by dissolving 20 mg (18.5 mmol) of $[CuI(pyridine)]_4$ in CH_2Cl_2 and adding 8.2 μL of 4-acetylpyridine (d = 1.095 g cm^{-3}, 74 mmol). After addition of *n*-hexane, precipitation of **4a** as a yellow powder took place. Single crystals of **4a** were obtained by crystallization at room temperature from CH_2Cl_2/pentane. Freshly produced batches of **4a** were routinely checked for pureness both analytically and by X-ray powder diffraction (XRPD) on a Bragg−Brentano Philips PW 1820 diffractometer (Cu Kα radiation, λ = 1.5418 Å) equipped with primary and secondary Soller slits (2.3°), divergence slit (1.0°), receiving slit (0.2 mm), and secondary beam graphite monochromator, performing θ:2θ step-scans in the range $3 < 2\theta < 35°$, with $\Delta 2\theta = 0.02°$ and t = 1 s step^{-1}. Anal. Calcd for C_7H_7NOCuI: C, 26.9; H, 2.2; N, 4.5. Found: C, 27.5; H, 2.4; N, 4.4.

Synthesis of $[CuI(4\text{-acetylpyridine})_2]_n$ (4b). Compound **4b** was prepared by adding 16.4 μL of 4-acetylpyridine (d = 1.095 g cm^{-3}, 148 mmol) to 20 mg (18.5 mmol) of $[CuI(pyridine)]_4$ dissolved in CH_2Cl_2. Red needles of **4b** were obtained by slow room-temperature evaporation of the solvent. Freshly produced batches of **4b** were checked for pureness both analytically and by XRPD, as described for **4a**. Anal. Calcd for $C_{14}H_{14}N_2O_2CuI$: C, 38.8; H, 3.2; N, 6.5. Found: C, 39.2; H, 3.4; N, 6.4.

Synthesis of $[CuCl(quinoline)]_n$, $[CuCl(2\text{-methylquinoline})]_n$, $[CuBr(pyridine)]_n$, $[CuBr(2,4,6\text{-trimethylpyridine})]_n$, $[CuBr(2\text{-methylquinoline})]_n$, and $[CuI(2,4,6\text{-trimethylpyridine})]_n$ (5−10). Compounds **5**−**10** were prepared according to literature methods.[10c,11e,h] Their freshly produced batches were checked for pureness both analytically and by XRPD as for **4a**.

Photoluminescence Measurements. Solid-state emission spectra were recorded using a Spex Fluorolog II spectrofluorometer equipped with a Hamamatsu R928A water-cooled photomultiplier tube.

NLO Kurtz−Perry Powder Measurements. The 1064-nm wavelength of a Nd:YAG pulsed laser beam (shifted, in the case of **4a** and **4b**, to 1907 nm by stimulated Raman scattering in a high-pressure hydrogen cell) was directed on sample-containing capillaries. The scattered SHG radiation was collected by an elliptical mirror, filtered in order to select only the second-order contribution and recollected with a Hamamatsu R5108 photomultiplier tube. SHG efficiencies were evaluated by taking, as a reference, the SH signal of urea or quartz for compounds **4a**, **4b** or **5**−**10**, respectively.

X-ray Structures of $[CuI(4\text{-acetylpyridine})]_n$ (4a) and $[CuI(4\text{-acetylpyridine})_2]_n$ (4b). Suitable crystals of **4a** and **4b** were mounted in air on the glass fiber tip of a goniometer head. Enraf Nonius CAD4 (**4a**) and Bruker SMART CCD area detector (**4b**) diffractometers, supplied with graphite-monochromatized Mo Kα radiation (λ = 0.710 73 Å), were used.

4a. Cell parameters and orientation matrix were determined from 25 accurately centered reflections. Data collection was performed by applying the ω-scan method, with fixed scan

(8) The reader can refer to, for example: (a) Healy, P. C.; Pakawatchai, C.; White, A. H. *J. Chem. Soc., Dalton Trans.* **1983**, 1917. (b) Dyason, J. C.; Engelhardt, L. M.; Healy, P. C.; White, A. H. *Aust. J. Chem.* **1984**, *37*, 2201. (c) Scramm, V.; Pierre, A.; Hiller, W. *Acta Crystallogr. Sect. C* **1984**, *40*, 1840. (d) Hiller, W. *Z. Naturforsh. Teil B* **1984**, *39*, 861. (e) Dyason, J. C.; Engelhardt, L. M.; Healy, P. C.; Pakawatchai, C.; White, A. H. *Inorg. Chem.* **1985**, *24*, 1950. (f) Fuller, M. W.; Costanzo, V.; Murray, K. S.; Black, D. St. C.; Hambley, T. W.; Snow, M. R. *Aust. J. Chem.* **1985**, *38*, 865. (g) Dyason, J. C.; Engelhardt, L. M.; Healy, P. C.; Pakawatchai, C.; White, A. H. *Inorg. Chem.* **1985**, *24*, 1950. (h) Rath, N. P.; Maxwell, J. L.; Holt, E. M. *J. Chem. Soc., Dalton Trans.* **1986**, 2449. (i) Healy, P. C.; Kildea, J. D.; Skelton, B. W.; Waters, A. F.; White, A. H. *Acta Crystallogr. Sect. C* **1991**, *47*, 1721.

(9) The reader is referred to, for example: (a) Raston, C. L.; White, A. H. *J. Chem. Soc., Dalton Trans.* **1976**, 2153. (b) Schramm, V. *Cryst. Struct. Commun.* **1980**, *9*, 1231. (c) Churchill, M. R.; Davies, G.; El-Sayed, M. A.; Hutchinson, J. P.; Rupich, M. W. *Inorg. Chem.* **1982**, *21*, 995. (d) Dyason, J. C.; Healy, P. C.; Engelhardt, L. M.; Pakawatchai, C.; Patrick, V. A.; Raston, C. L; White, A. H. *J. Chem. Soc., Dalton Trans.* **1985**, 831. (e) Healy, P. C.; Pakawatchai, C.; Raston, C. L.; Skelton, B. W.; White, A. H. *J. Chem. Soc., Dalton Trans.* **1983**, 1905. (f) Engelhardt, L. M.; Healy, P. C.; Kildea, J. D.; White, A. H. *Aust. J. Chem.* **1989**, *42*, 107. (g) Sugahara, E.; Paula, M. M. S.; Vencato, I.; Franco, C. V. *J. Coord. Chem.* **1996**, *39*, 59.

(10) The reader can refer to, for example: (a) Campbell, J. A.; Raston, C. L.; White, A. H. *Aust. J. Chem.* **1977**, *30*, 1937. (b) Pakawatchai, P. C.; Raston, C. L.; Skelton, B. W.; White, A. H. *J. Chem. Soc., Dalton Trans.* **1983**, 1905. (c) Healy, P. C.; Kildea, J. D.; Skelton, B. W.; White, A. H. *Aust. J. Chem.* **1989**, *42*, 115. (d) Engelhardt, L. M.; Healy, P. C.; Kildea, J. D.; Skelton, B. W.; White, A. H. *Aust. J. Chem.* **1989**, *42*, 933.

(11) The reader is referred to, for example: (a) Campbell, J. A.; Raston, C. L.; White, A. H. *Aust. J. Chem.* **1977**, *30*, 1937. (b) Eitel, E.; Oelkrug, D.; Hiller, W.; Strahle, J. *Z. Naturforsh. Teil B* **1980**, *35*, 1247. (c) Goher, M. A. S.; Mak, T. C. W. *Inorg. Chim. Acta* **1985**, *L27*, 101. (d) Rath, N. P.; Maxwell, J. L.; Holt, E. M. *J. Chem. Soc., Dalton Trans.* **1986**, 2449. (e) Healy, P. C.; Kildea, J. D.; Skelton, B. W.; White, A. H. *Aust. J. Chem.* **1989**, *42*, 93. (f) Engelhardt, L. M.; Healy, P. C.; Kildea, J. D.; White, A. H. *Aust. J. Chem.* **1989**, *42*, 185. (g) Engelhardt, L. M.; Healy, P. C.; Kildea, J. D.; Skelton, B. W.; White, A. H. *Aust. J. Chem.* **1989**, *42*, 933. (h) Healy, P. C.; Skelton, B. W.; Waters, F.; White, A. H. *Aust. J. Chem.* **1991**, *44*, 1049.

(12) (a) Kyle, K. R.; Ryu, C. K.; DiBenedetto, J.; Ford, P. C. *J. Am. Chem. Soc.* **1991**, *113*, 2954. (b) Vitale, M.; Palke, W. E.; Ford, P. C. *J. Phys. Chem.* **1992**, *96*, 8329.

(13) Cariati, E.; Xianhui Bu; Ford, P. C. *Chem. Mater.* **2000**, *12*, 3385.

(14) Healy, P. C.; Kildea, J. D.; Skelton, B. W.; White, A. H. *Aust. J. Chem.* **1989**, *42*, 93.

Table 1. Crystallographic Data and Refinement Details for [CuI(4-acetylpyridine)]$_n$ (4a) and [CuI(4-acetylpyridine)$_2$]$_n$ (4b)

	4a	4b
formula	C_7H_7NOCuI	$C_{14}H_{14}N_2O_2CuI$
formula wt, g mol^{-1}	311.58	432.75
crys color, habit, and size, mm	orange, needle, 0.32 × 0.12 × 0.10	red, plate, 0.48 × 0.24 × 0.20
crystal system	orthorhombic	monoclinic
space group	$P2_12_12_1$	Pc
a, Å	4.121(4)	12.374(1)
b, Å	8.376(4)	4.251(4)
c, Å	26.321(10)	15.081(1)
β, deg		106.67(1)
V, Å^3	908.5(2)	759.9(2)
Z	4	2
ρ_{calcd}, Mg m^{-3}	2.278	1.891
temperature, K	298(2)	193(2)
λ, Å	0.71073	0.71073
μ (Mo Kα), mm^{-1}	5.74	3.47
R(int)[a]	0.0416	0.0236
F(000)	584	420
data collection θ range, deg	3.0 ≤ θ ≤ 25.0	1.7 ≤ θ ≤ 30.2
measured reflections	1930	8591
unique reflections	1564	2363
refinement method	full-matrix least squares on F^2	full-matrix least squares on F^2
data, restraints, params	1564, 0, 100	4011, 2, 181
goodness of fit $S(F^2)$	1.064	0.769
final $R(F)$ and $wR(F^2)$ for $I > 2\sigma$[a]	0.0362, 0.0926	0.0192, 0.0395
final $R(F)$ and $wR(F^2)$ for all data	0.0395, 0.0926	0.0280, 0.0395
largest diff peak and hole, e Å^{-3}	1.21, −1.20	0.63, −0.25

[a] $R(\text{int}) = \sum|F_o^2 - F_{mean}^2|/\sum|F_o^2|$; $S(F^2) = [\sum w(F_o^2 - F_c^2)^2/(n-p)]^{1/2}$; $R(F) = \sum||F_o| - |F_c||/\sum|F_o|$; $wR(F^2) = [\sum w(F_o^2 - F_c^2)^2/\sum wF^4]^{1/2}$; $w = 1/[\sigma^2(F_o^2) + (0.019P)^2 + 1.88P]$ with F_o and F_c observed and calculated structure factors, respectively, n and p number of reflections and refined parameters, respectively, and $P = (F_o^2 + 2F_c^2)/3$.

speed and variable scan range [(1.3 + 0.35 tan θ)°] within the sphere 3° < θ < 25°. No significant variation in the intensities of three separate reflections was observed. Data reduction afforded 1930 reflections, 1564 unique. Integrated reflections were empirically corrected for absorption, Lorentz, and polarization effects.

4b. Cell parameters and orientation matrix were obtained from 136 accurately centered reflections. A total of 1818 frames were measured by applying the ω-scan method with $\Delta\omega = 0.3°$, 35 s per frame, and sample−detector distance fixed at 3.864 cm. Data reduction, performed within the sphere $2\theta < 70°$, afforded 8591 reflections, 2363 unique. An empirical absorption correction was applied to the integrated reflections.[15]

The structures were solved by direct methods[16] and successfully refined with full-matrix least-squares calculations.[17] Anisotropic temperature factors were assigned to all atoms but hydrogens, which were made riding their parent atoms with a common isotropic displacement parameter, arbitrarily chosen as 1.2 times that of the pertinent parent carbon. Crystallographic data and refinement details for both compounds are reported in Table 1. Selected bond lengths and angles are gathered in Tables 2 and 3.

(15) Sheldrick, G. M. *SADABS: program for empirical absorption correction*; University of Göttingen: Göttingen, Germany, 1996.

(16) Altomare, A.; Cascarano, G.; Giacovazzo, C.; Guagliardi, A.; Moliterni, A. G. G.; Burla, M. C.; Polidori, G.; Camalli, M.; Spagna, R. *SIR97: package for structure solution by direct methods*; University of Bari: Bari, Italy, 1997.

(17) Sheldrick, G. M. *SHELX97*: *program for crystal structure refinement*; University of Göttingen: Göttingen, Germany, 1997.

Table 2. Selected Bond Lengths (Å) and Angles (deg) for [CuI(4-acetylpyridine)]$_n$ (4a)[a]

I−Cu	2.672(2)	Cu−I−Cu#3	101.84(7)
I−Cu#1	2.637(2)	Cu−I−Cu#4	65.76(4)
I−Cu#2	2.6525(14)	C(1)−N(1)−Cu	122.1(5)
Cu−N(1)	2.046(7)	C(5)−N(1)−Cu	121.5(5)
N(1)−C(1)	1.345(9)	C(5)−N(1)−C(1)	116.4(7)
N(1)−C(5)	1.325(11)	N(1)−C(1)−C(2)	123.6(8)
C(1)−C(2)	1.350(11)	C(1)−C(2)−C(3)	119.7(7)
C(2)−C(3)	1.391(12)	C(4)−C(3)−C(2)	117.4(8)
C(3)−C(4)	1.383(11)	C(4)−C(3)−C(6)	119.2(8)
C(3)−C(6)	1.499(11)	C(2)−C(3)−C(6)	123.3(7)
C(4)−C(5)	1.373(12)	C(5)−C(4)−C(3)	118.5(8)
C(6)−O(1)	1.210(12)	N(1)−C(5)−C(4)	124.4(7)
C(6)−C(7)	1.474(12)	O(1)−C(6)−C(7)	121.3(8)
I#1−Cu−I	101.84(7)	O(1)−C(6)−C(3)	119.1(9)
I#1−Cu−I#2	114.58(5)	C(7)−C(6)−C(3)	119.6(8)
I#2−Cu−I	113.40(5)		

[a] Symmetry operations applied to generate equivalent atoms: #1 ($x - 1, y, z$); #2 ($x - 1/2, -y + 3/2, -z + 2$); #3 ($x + 1, y, z$); #4 ($x + 1/2, -y + 3/2, -z + 2$).

Table 3. Selected Bond Lengths (Å) and Angles (deg) for [CuI(4-acetylpyridine)$_2$]$_n$ (4b)[a]

I−Cu	2.6209(17)	I−Cu−I#2	108.05(5)
Cu−I#2	2.6320(17)	C(15)−N(1)−C(11)	117.1(3)
Cu−N(1)	2.081(3)	C(15)−N(1)−Cu	121.9(2)
Cu−N(2)	2.088(3)	C(11)−N(1)−Cu	120.3(2)
N(1)−C(15)	1.337(4)	N(1)−C(11)−C(12)	123.2(3)
N(1)−C(11)	1.344(4)	C(11)−C(12)−C(13)	119.3(3)
C(11)−C(12)	1.385(5)	C(12)−C(13)−C(14)	118.0(3)
C(12)−C(13)	1.387(5)	C(12)−C(13)−C(16)	122.6(3)
C(13)−C(14)	1.392(4)	C(14)−C(13)−C(16)	119.4(3)
C(13)−C(16)	1.510(4)	C(15)−C(14)−C(13)	118.8(3)
C(14)−C(15)	1.390(5)	N(1)−C(15)−C(14)	123.5(3)
C(16)−O(1)	1.214(4)	O(1)−C(16)−C(17)	121.5(3)
C(16)−C(17)	1.496(5)	O(1)−C(16)−C(13)	119.7(3)
N(2)−C(21)	1.324(4)	C(17)−C(16)−C(13)	118.8(3)
N(2)−C(25)	1.339(4)	C(21)−N(2)−C(25)	117.0(3)
C(21)−C(22)	1.374(5)	C(21)−N(2)−Cu	120.5(2)
C(22)−C(23)	1.391(5)	C(25)−N(2)−Cu	121.8(2)
C(23)−C(24)	1.385(4)	N(2)−C(21)−C(22)	124.4(3)
C(23)−C(26)	1.512(5)	C(21)−C(22)−C(23)	118.4(3)
C(24)−C(25)	1.391(5)	C(24)−C(23)−C(22)	118.1(3)
C(26)−O(2)	1.207(4)	C(24)−C(23)−C(26)	119.3(3)
C(26)−C(27)	1.507(5)	C(22)−C(23)−C(26)	122.5(3)
Cu−I−Cu#1	108.05(5)	C(23)−C(24)−C(25)	118.8(3)
N(1)−Cu−N(2)	102.20(10)	N(2)−C(25)−C(24)	123.0(3)
N(1)−Cu−I	115.64(8)	O(2)−C(26)−C(27)	121.8(4)
N(2)−Cu−I	109.44(8)	O(2)−C(26)−C(23)	120.0(3)
N(1)−Cu−I#2	107.96(9)	C(27)−C(26)−C(23)	118.1(3)
N(2)−Cu−I#2	113.65(8)		

[a] Symmetry operations applied to generate equivalent atoms: #1 ($x, y - 1, z$); #2 ($x, y + 1, z$).

Results and Discussion

Novel CuI/4-acetylpyridine Adducts: Synthesis, Solid-State Second-Order NLO Responses, and Structural Aspects. Addition of different amounts of acpy (acpy = 4-acetylpyridine) to a CH_2Cl_2 solution of [CuI(pyridine)]$_4$ followed by slow evaporation of the solvent yielded two distinct crystalline products (**4a** and **4b**, with stoichiometric ratios [CuI]/[acpy] 1 and 0.5, respectively). To investigate their second-order NLO activity, Kurtz−Perry powder method measurements[18] were performed with a nonresonant incident wavelength of 1907 nm (as **4a** and **4b** do not absorb above 600 nm). Both materials proved to be second harmonic generators. Indeed, while **4a** is modestly so, **4b** behaves more promisingly: SHG efficiencies about 1 and 14 times that of urea, respectively, have been recorded.[19]

(18) Kurtz, S. K.; Perry, T. T. *J. Appl. Phys.* **1968**, *39*, 3798.

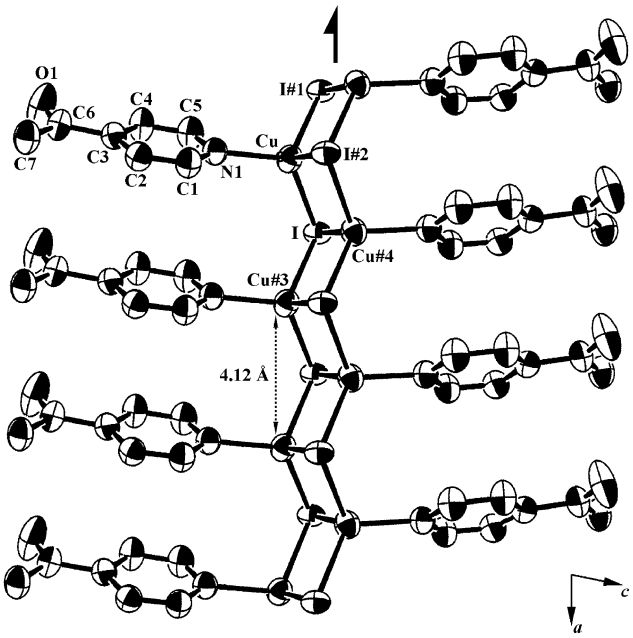

Figure 1. Representation (with 50% probability, Ortep) of the double-stranded stair, structural motif for **4a**. Hydrogen atoms have been omitted for clarity. The labeling scheme was adopted throughout the paper.

Such a different SHG efficiency being possibly of structural origin, single-crystal X-ray structure determinations were performed on both compounds (see Experimental Section). Recrystallization of **4a** from CH_2Cl_2/pentane yielded suitable needles for room-temperature data collection. The resulting structure is consistent with the [Cu:I:acpy] = [1:1:1] stoichiometry. By means of Cu−I bonds, the [CuI(acpy)] asymmetric units arrange in polymeric $[CuI(acpy)]_n$ double-stranded stairs (Figure 1), a structural motif already encountered for a certain number of $[CuX(L)]_n$ complexes (X = Cl, Br, or I) with manifold substituted pyridines (L).[11] In the present case, the stairs grow along *a* as 2_1 "degenerate helixes" of pitch *a* (4.12 Å). As already reported for stairs bearing planar, pseudoaromatic ligands,[14] a certain distortion from an "ideal ladder" (i.e., from "perfectly orthogonal" steps) occurs, I−Cu−I angles along the translation axis being 101.8°. A herringbone motif, described by the reciprocal packing of the stairs, is appreciable on viewing the structure normally to the [1 0 0] plane (Figure 2).

Copper ions, in distorted tetrahedral geometry, are bound to three μ^3-iodines and the nitrogen of one organic ligand. As can be drawn from Table 4, the Cu−I, Cu−I#1, Cu−I#2, and Cu−N(1) distances (see Figure 1 for highlights on the labeling scheme), 2.67, 2.64, 2.65, and 2.04 Å, respectively, are in agreement with the mean values shown for the same parameters by known $[CuI(L)]_n$ stairs (2.71, 2.64, 2.67, and 2.05 Å, respectively).[20] The Cu···Cu#4 diagonal interaction (2.89 Å, Table 4) is

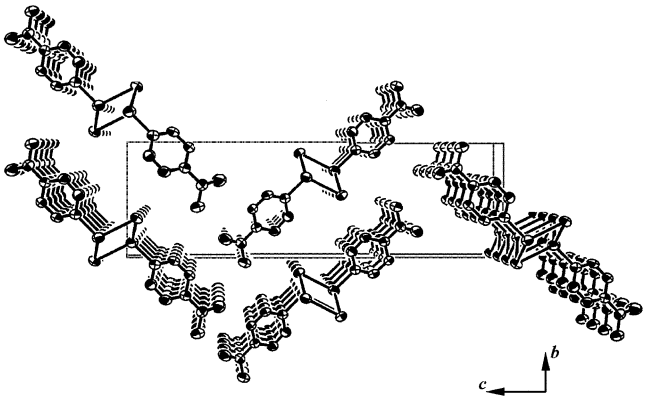

Figure 2. Representation (with 50% probability, Ortep) of the structure of **4a** normally to the [1 0 0] plane. A herringbone motif, described by the reciprocal packing of the stairs, can be appreciated. Hydrogen atoms have been omitted for clarity.

Table 4. Comparison of Selected Bond Distances (Å) in Compound $[CuI(4\text{-acetylpyridine})]_n$ (4a) and in Known $[CuI(L)]_n$ 'Stairs'

compound	Cu···Cu#4[a]	I···I#2[a]	Cu−I[a]	Cu−I#1[a]	Cu−I#2[a]	Cu−N(1)[a]
4a	2.89	4.47	2.67	2.64	2.65	2.04
$[CuI(L)]_n$ stairs	3.07[b]	4.35[b]	2.71[b]	2.64[b]	2.67[b]	2.05[b]

[a] Consult Figure 1 for highlights on the labeling scheme. #1 ($x - 1, y, z$); #2 ($x - {}^1/_2, -y + {}^3/_2, -z + 2$); #4 ($x + {}^1/_2, -y + {}^3/_2, -z + 2$). [b] Mean value from selected stairs.[20]

greater than the sum of the van der Waals radii (2.80 Å), thus precluding the formation of significant "metal cluster centered" orbitals.[6] The halides, tricoordinated in distorted pyramidal geometry, show a I···I2# diagonal distance of 4.47 Å, again comparable to the mean value observed in other $[CuI(L)]_n$ stairs (4.35 Å, Table 4).[20] The organic moiety is approximately planar, the root mean square (rms) of the distance of its non-hydrogen atoms from its least-squares plane being 0.02 Å. The ligands are stacked along both sides of the Cu−I skeleton, their least-squares planes being at a distance of 3.65 Å.

Compound **4b**, obtained by performing the reaction with excess ligand, is unstable when left in air in open vials; as confirmed by X-ray powder diffraction, it slowly transforms into poorly crystalline **4a**. No transformation is, however, observed when **4b** is kept sealed.

Suitable crystals were obtained by slow evaporation of the solvent. The low-temperature X-ray data collection confirmed the [Cu:I:acpy] = [1:1:2] stoichiometry. Copper and iodine atoms are arranged alternately along "zigzag single-stranded chains" (Figure 3) extending along the monoclinic axis with a translation step of 4.25 Å. The presence of two independent ligands on every metal (1 and 2 in Figure 3) results in the rare $[CuX(L)_2]_n$ motif, encountered previously just in $[CuCl(HNA)_2]_n$ (HNA = nicotinic acid).[21] Compounds of stoichiometry $[CuX(L)_2]$ usually exist either as bis(μ-halo)bridged dimers with a $[CuI]_2$ rhombohedral core[8i] or as distorted trigonal planar monomers.[7d]

Along the chain, copper ions are tetracoordinated, with distorted tetrahedral arrangement, by two μ^2-iodines and the nitrogen atoms of two independent

(19) No measurements have been performed on the Cu(I) polymeric materials investigated in this work to ascertain their response as a function of grain size.

(20) The mean values reported in Table 4 have been determined on averaging the structural parameters of the $[CuI(L)]_n$ stairs (L = pseudoaromatic η^1-nitrogen donor ligand) present in the 2001 release of the Cambridge Structural Database [*ConQuest, V. 1.3*; Cambridge Crystallographic Data Centre (CCDC), 2001]. Their Ref. Codes follow: Cuipys Falyew, Falyia, Kalmuf, Kalnoa, Sawtoz, and Sawtuf.

(21) Goher, M. A. S.; Mak, T. C. W. *Inorg. Chim. Acta* **1987**, *127*, L13−L16.

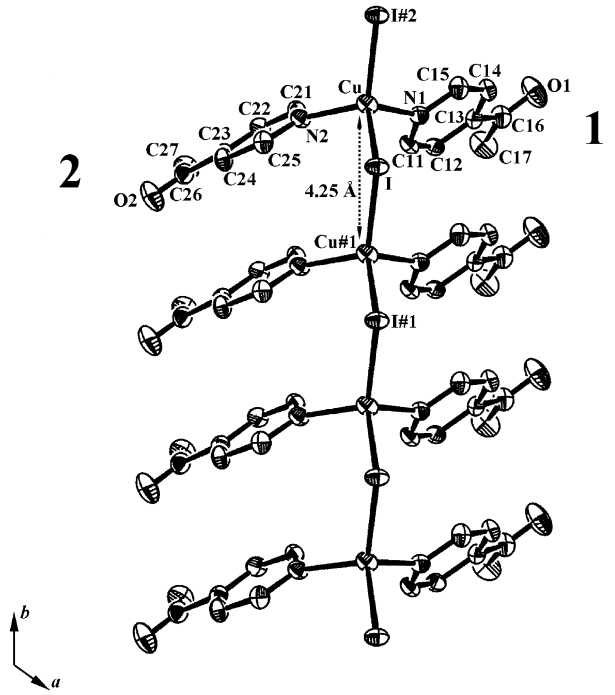

Figure 3. Representation (with 50% probability, Ortep) of the zigzag single-stranded chain, structural motif for **4b**. Hydrogen atoms have been omitted for clarity. The labeling scheme was adopted throughout the paper.

Table 5. Comparison of Selected Bond Distances (Å) in Compound [CuI(4-acetylpyridine)$_2$]$_n$ (4b) and in Known [CuI(L)]$_n$ 'Chains'

compound	Cu···Cu#1[a]	I···I#2[a]	Cu−I[a]	Cu−I#2[a]	Cu−N[a]
4b	4.25	4.25	2.63	2.62	2.08[b]
[CuI(L)]$_n$ chains	4.13[c]	4.13[c]	2.57[c]	2.51[c]	2.01[c]

[a] Consult Figure 3 for highlights on the labeling scheme. #1 (x, $y-1$, z); #2 (x, $y+1$, z). [b] Mean value of the Cu−N(1) and Cu−N(2) distances in **4b**. [c] Mean value from selected chains.[22]

organic ligands. The Cu−I/I#2 and Cu−N(1)/N(2) vectors departing from the same metal center (see Figure 3 for highlights on the labeling scheme) have values of 2.63/2.62 and 2.08/2.09 Å, respectively. As clearly emerging from Table 5, the latter parameters are retraceable to those of reported [CuI(L)]$_n$ chains;[22] i.e., they do not seem significantly affected by the presence of two (rather than one) independent ligands. As in known [CuI(L)]$_n$ chains,[22] even in **4b** the minimum intermetal distance (4.13 vs 4.25 Å, respectively; Table 5) is abundantly greater than the van der Waals radii. The halide, bridging two consecutive metals, has digonal bent geometry with an I···I#2 minimum contact of 4.25 Å (to be compared with that of 4.13 Å reported in Table 5 for renown [CuI(L)]$_n$ chains).[22] The organic ligands are approximately planar, the rms's of the distance of the non-hydrogen atoms from their least-squares planes being 0.04 and 0.03 Å for ligands 1 and 2, respectively. Both ligands stack along the Cu−I skeleton with a distance, among consecutive least-squares planes, of 3.75 and 3.40 Å, respectively.

(22) The mean values reported in Table 5 have been determined on averaging the structural parameters of the [CuI(L)]$_n$ chains (L = pseudoaromatic η^1-nitrogen donor ligand) present in the 2001 release of the Cambridge Structural Database [*ConQuest, V. 1.3*; Cambridge Crystallographic Data Centre (CCDC), 2001]. Their Ref. Codes follow: Cerhem, Cuicol10, Felcee, Sawwes, and Veftef.

Novel CuI/4-acetylpyridine Adducts: Solid-State Emissive Properties. When excited at 350 nm, **4a** shows a single intense emission centered at 612 nm (Table 6). The latter is rather red-shifted with respect to the emission of the structurally related [CuI(pyridine)]$_n$ stair (**1**), centered at 437 nm (Table 6) and attributed to a decay from a triplet halide-to-ligand charge-transfer excited state ($p_X \rightarrow \pi_L^*$, ^{3}XLCT*).[6] If the bathochromic shift observed for **4a** were ascribed to the lowering of the π_L^* energy level promoted by the electron-withdrawing acetyl group, the emission of **4a** could still be retraced to a ^{3}XLCT* decay. This latter hypothesis can be supported by the emission of the structurally related [CuI(3-pyridinealdoxime)]$_n$ stair[23] (bearing as well an electron-withdrawing group on the ligand), which, when excited at 350 nm, shows a single intense emission centered at 550−560 nm.

However, the above bathochromic shifts are unexpectedly pronounced to be completely attributed to the energetic stabilization of the π_L^* levels allowed by modest electron-withdrawing groups such as acetyl or aldoxime ones: for the sake of completeness, it must be pointed out that the emission maximums recorded for **4a** and [CuI(3-pyridinealdoxime)]$_n$ could as well be consistent with a ^{3}MLCT* process.

When excited at 350 nm, **4b** shows an emission band centered around 700 nm (Table 6). The emissive properties of [CuX(L)$_m$]$_n$ single-stranded chains ($m = 1$ or 2) have never been previously described. In analogy to the few studies on the photoluminescence of CuI/L stairs,[6] it can be tentatively suggested that the excited-state responsible for the emission of **4b** is ^{3}XLCT* in character.

Novel CuI/4-acetylpyridine Adducts: Solid-State Second-Order NLO Responses. Table 6 collects the SHG efficiencies for **4a** and **4b** [SHG(n), n = **4a**, **4b**], measured on their powders by the Kurtz−Perry technique[18] working with a nonresonant incident wavelength of 1907 nm and taking urea as reference (see Experimental Section). The rather large difference in their SHG performances [SHG(**4b**)/SHG(**4a**) ∼14] prompted us to investigate the electronic processes and the structural aspects that could be at the origin of their second-order nonlinear optical activity. According to the so-called "two-level model",[24] molecular second-order NLO responses are mainly dictated by one major charge-transfer process. In the solid state, the latter is somehow "modulated" by the reciprocal arrangement of the individual moieties. This modulation was brilliantly rationalized by Zyss[25] through geometrical relationships linking the contribution of the molecular quadratic hyperpolarizability along the CT axis (β_{CT}) to the components of the crystalline nonlinearity per molecule (b_{eff}). Thus, to rationalize the solid-state NLO behavior of **4a** and **4b**, a comparison of their experimental SHGs to the phase-matchable components of b_{eff} was carried on through the Zyss formulas. To develop a "prejudice-

(23) Aakeröy, C. B.; Beatty, A. M.; Leinen, D. S.; Lorimer, K. R. *Chem. Commun.* **2000**, 935.

(24) (a) Oudar, J. L.; Chemla, D. S. *J. Chem. Phys.* **1977**, *66*, 446. (b) Oudar, J. L. *J. Chem. Phys.* **1977**, *67*, 2664.

(25) (a) Zyss, J.; Oudar, J. L. *Phys. Rev. A* **1982**, *26*, 2028. (b) Zyss, J.; Chemla, D. S. In *Nonlinear Optical Properties of Organic Molecules and Crystals*; Chemla, D. S., Zyss, J., Eds.; Academic Press Inc.: Orlando, FL, 1987; Vol. 1, pp 23−187.

Table 6. Halide, Ligand, Stoichiometry, Structural Motif, Crystallographic Class, Copper···Copper Minimum Distance, Photoluminescence Emission Maximum, Powder Efficiency in Second Harmonic Generation, Angles from the ^{3}MLCT* Axis to Proper (According to Point Symmetry) Crystallographic Axes, and b_{eff} (β_{CT} Taken as Unity) for 1−10

	X	L[a]	stoich	motif	cryst Cl	d_{Cu-Cu} (Å)	λ^{em}_{max}(nm)	SHG	θ (deg)	ϕ (deg)	b_{eff}
1	I	py	$[CuX(L)]_n$	stair	2/*m*	2.88	437	*b*	*b*	*b*	*b*
4a	I	acpy	$[CuX(L)]_n$	stair	222	2.89	612	1[c]	63.3	22.5	0.050
4b	I	acpy	$[CuX(L)_2]_n$	chain	m	4.25	∼700	14 [c]	∼52[e]	any	0.300
5	Cl	quin	$[CuX(L)]_n$	stair	222	3.07	602	negligible[d]	20.0	66.5	0.040
6	Cl	quind	$[CuX(L)]_n$	chain	222	3.80	590	2.3[d]	66.2	23.2	0.122
7	Br	py	$[CuX(L)]_n$	stair	2	2.91	509	negligible[d]	62.2	any	0.365
8	Br	trimeth	$[CuX(L)]_n$	chain	*m*2*m*	3.96	418, 536	22.5[d]	13.9	65.5	0.009
9	Br	quind	$[CuX(L)]_n$	chain	*m*2*m*	3.90	645	7.5[d]	0.7	66.2	0.001
10	I	trimeth	$[CuX(L)]_n$	chain	2*mm*	4.16	443, 535	45.0[d]	20.6	0	0

[a] py = pyridine; acpy = 4-acetylpyridine; quin = quinoline; quind = 2-methylquinoline; trimeth = 2,4,6-trimethylpyridine. [b] Unavailability because of centrosymmetric space group. [c] Measured at an incident wavelength of 1907 nm with respect to urea. [d] Measured at an incident wavelength of 1064 nm with respect to quartz. [e] See text for a detailed description.

free" comparison, any contribution from either the literature or the spectroscopic acquisitions described in the previous sections were disregarded. In this context, the presence of metal-bound pyridines para-substituted with electron-withdrawing groups may suggest the relevance of a charge-transfer electronic transition from the metal occupied d orbitals to the empty π_L* system of the ligand ($d_{Cu} \rightarrow \pi_L$*, ^{3}MLCT*). The latter hypothesis is supported by some Ir(I), Rh(I), and Os(II) compounds bearing similar ligands, for which the relevance of a ^{3}MLCT* on their second-order NLO response was successfully proposed.[26] Zyss relationships were thus applied: (i) adopting an "oriented gas" model, i.e., supposing that weak interactions are the only intermolecular forces present; (ii) assuming **4a** and **4b** as monodimensional systems in which the unique axis is lying along the CT direction; (iii) giving to the CT an M → L character, i.e., modeling the CT axis with the Cu−N vector. The angles needed to evaluate b_{eff} were thus measured considering the reciprocal orientation of the Cu−N vectors and the proper crystallographic axes. Crystallographic classes, angles defining the CT axes orientation within the crystal, and calculated b_{eff}'s for **4a** and **4b** are reported in Table 6.

The 222 point symmetry of **4a** is one of the least likely to give valuable bulk susceptibilities: nevertheless, the *effective* b_{eff}, $\sin(\phi)\cos(\phi)\cos(\theta)\sin^2(\theta)\beta_{CT}$, has to be estimated by taking into account the *actual* orientation of the ^{3}MLCT*, i.e., the *actual* θ and ϕ angles from the assumed CT axis to *a* and *c*, respectively, their values being 63.3° and 22.5° (vs ideal ones of 54.7° and 45.0°), b_{eff}(**4a**) = $0.050\beta_{CT}$(**4a**).

For **4b**, belonging to crystallographic class *m*, $b_{eff} = \sin(\theta)\cos^2(\theta)\beta_{CT}$, θ is the angle between the ^{3}MLCT* and the monoclinic axes. With two aromatic ligands on each copper ion, the building up of an extended π_L*-acceptor system involving both of them may be reasonably supposed. Since the Cu−N(1)/N(2) vectors intersect the monoclinic axis at angles of 51.8° and 52.6°, respectively, the *effective* ^{3}MLCT* axis, spanning the whole extended π_L*-system, forms, with the monoclinic axis, a similar angle as well (∼52° vs the ideal one of 35.3°). This value results in a b_{eff}(**4b**) of $\sim 0.300\beta_{CT}$(**4b**).

Assuming β_{CT}(**4a**) almost identical to β_{CT}(**4b**) (an acceptable approximation considering that M and L are in both cases the same), comparison of the experimental SHG(**4b**)/SHG(**4a**) ratio (∼14) to the calculated b_{eff}(**4b**)/b_{eff}(**4a**) one (∼6) gives indirect evidence of the inadequacy of a ^{3}MLCT* *alone* to explain the electronic origin of the second-order NLO response for **4a** and **4b**. Indeed, to justify their emissive properties, charge-transfer transitions *involving the bridging halides* were taken into consideration (see previous section); thus, to attempt a rationalization of both their NLO activities and their emissions, a more complete and extended series of experimental data became necessary. We consequently investigated the photoluminescence emissions and the second-order NLO responses of a series of structurally known noncentrosymmetric [CuX(L)] (X = Cl, Br, I) chains and stairs with pseudoaromatic η^1-nitrogen donor ligands (L).

Known Acentric Chain and Stair Adducts of Cu(I) with Various Pseudoaromatic η^1-Nitrogen Donor Ligands: Solid-State Emissive Properties. We studied the emissive properties of a series of structurally related $[CuX(L)]_n$ polymeric materials (**5**−**10**) with chain or stair motifs (X = Cl, Br, or I; L = pyridine, 2,4,6-trimethylpyridine, quinoline, or 2-methylquinoline).[10c,11e,h] Their structural motifs, solid-state emission maximums (λ^{em}_{max}) and minimum copper···copper distances are summarized in Table 6.

The stair $[CuBr(pyridine)]_n$ (**7**) shows a broad emission centered at 509 nm, quite red-shifted with respect to that at 437 nm of $[CuI(pyridine)]_n$ (**1**), assigned to a decay from a ^{3}XLCT* process.[6] Unexpectedly, such a shift does not follow the halide polarizability trend (I > Br). A broad band centered at 602 nm dominates the emission spectrum of another stair compound, $[CuCl(quinoline)]_n$ (**5**). Given both the structural motif and the large Cu···Cu distances (3.07 and 2.91 Å, for **5** and **7**, respectively; Table 6), it seems reasonable, in both cases, to discard any participation of metal-delocalized orbitals.[6] With λ^{em}_{max} being modulated by the nature of X, an influence of the halide on the CT processes controlling the emissions of **1**, **5**, and **7** appears plausible. Yet, the trend λ^{em}_{max}(**5**) > λ^{em}_{max}(**7**) > λ^{em}_{max}(**1**) does contrast that of the halides' polarizabilities or the ionization potentials. Such behavior was already encountered for some tetranuclear $[CuX(L)]_4$ species [X = Cl or I; L = 2-(diphenylmethyl)pyridine], whose chloro derivative emits, at room temperature, at significantly

(26) Roberto, D.; Ugo, R.; Bruni, S.; Cariati, E.; Cariati, F.; Fantucci, P. C.; Invernizzi, I.; Quici, S.; Ledoux, I.; Zyss, J. *Organometallics* **2000**, *19*, 1775.

lower energies than the iodo one.[27] These latter and our observations seem not to match with the ^{3}XLCT* hypothesis.[6] However, it is worth recalling that, according to ab initio calculations on $[CuX]_4$ clusters, the halide ionicity *within the cluster* follows the trend of the halide ionization potentials, I < Br < Cl:[27,28] $[CuX]_4$ coordinated iodine is less negatively charged than chlorine, this compensating for the lower ionization potential of the former and explaining the observed emission trend. If the above conclusions were extended to **1**, **5**, and **7**, we could reasonably explain why their ^{3}XLCT* energies do not respect an order merely based on the halides' polarizabilities.

A higher complexity characterizes the emissive behavior of the studied chain structures. The two related chains, $[CuCl(2\text{-methylquinoline})]_n$ (**6**) and $[CuBr(2\text{-methylquinoline})]_n$ (**9**), show solid-state emission bands at 590 and 645 nm, respectively (Table 6). No rationalization has been attempted up to now on chain solid-state room-temperature emission properties. The present Cu···Cu contacts (3.80 and 3.90 Å for **6** and **9**, respectively; Table 6) seem to preclude, even in this case, a "metal cluster centered" contribution,[6] but a well-founded discrimination between the ^{3}XLCT* and ^{3}MLCT* processes is, however, beyond reach. In favor of the first, it should be noted that, L being the same, the position of λ_{max}^{em} for **6** and **9** varies with the nature of X and, in this case, correlates with the halide's polarizability. Two distinct emissions are observed for the two related chains, $[CuBr(2,4,6\text{-trimethylpyridine})]_n$ (**8**) and $[CuI(2,4,6\text{-trimethylpyridine})]_n$ (**10**) (λ_{max}^{em} = 418, 536 nm, "structured", and 443, 535 nm, respectively; Table 6). Their LE emission is comparable to that of the stair structure **6** or **9** but at higher energy than in the chain **4b**.

Known Acentric Chain and Stair Adducts of Cu(I) with Various Pseudoaromatic η^1-Nitrogen Donor Ligands: Solid-State Second-Order NLO Responses. We investigated the second-order NLO properties of **5**−**10** by the Kurtz−Perry technique,[18] working on their powders with an incident nonresonant wavelength of 1064 nm and taking quartz as the reference (see Experimental Section). The resulting SHG efficiencies are collected in Table 6. For **7**, **8**, and **10**, since their emission maximums are close to 532 nm, a contribution from photoluminescence to SHG measured intensities cannot be totally excluded. Nevertheless, the trend of their SHG efficiencies does not follow that of the intensity of their emissions, thus excluding the fact that the SHGs are completely due to photoluminescence.

Applying the Zyss relationships,[25] we attempted to state whether the origin of the NLO efficiencies of **5**−**10** could be attributed to a ^{3}MLCT* process. Table 6 gathers their crystallographic classes, angles defining the ^{3}MLCT* axes orientation within the crystal, and calculated b_{eff}'s. As for the 4-acetylpyridine adducts, the direction of the Cu → π_L* CT transition was taken along the Cu−N bond.

Focus how attention on the stair **5** and the chain **6**, whose asymmetric units bear the same halide but *slightly* different organic ligands. Assigning to **5** and **6** the same β_{CT}, i.e., disregarding the small electronic contribution of the CH_3 group of 2-methylquinoline to the first hyperpolarizability, a comparison between SHG(**5**)/SHG(**6**) and b_{eff}(**5**)/b_{eff}(**6**) may be done. As both compounds have point symmetry 222, $b_{eff}(\mathbf{5},\mathbf{6}) = \sin(\phi)\cos(\phi)\cos(\theta)\sin^2(\theta)\beta_{CT}$ (θ and ϕ defined as for **4a**). Since $\theta(\mathbf{5}) = 20.0°$, $\theta(\mathbf{6}) = 66.2°$, $\phi(\mathbf{5}) = 66.5°$, and $\phi(\mathbf{6}) = 23.2°$, a nonvanishing b_{eff}(**5**)/b_{eff}(**6**) ratio [$b_{eff}(\mathbf{5}) = 0.040\beta_{CT}$ and $b_{eff}(\mathbf{6}) = 0.122\beta_{CT}$], contrasting with the experimental SHG(**5**)/SHG(**6**) one (Table 6), is obtained. Once again, we have indirect evidence that the ^{3}MLCT* process *alone* does not control the second-order NLO response of the subject compounds. It should, however, be mentioned that one more variable, namely, the structural motif, is involved in the **5** versus **6** comparison. Actually, as the two stairs **5** and **7** are the only SHG-inactive species, it could be supposed that, independently from the nature of the charge-transfer process, the stair motif is responsible for the macroscopic vanishing of the NLO activity. This hypothesis is also supported by the small NLO activity of the stair **4a** in comparison to that of **4b**. In other words, $[CuX(L)]_n$ chains always show larger NLO responses than the corresponding stairs.

The adduct **6** may be compared as well to **9**, with the same chain structural motif but different halides. The presence of the same organic moiety makes the assumption $\beta_{CT}(\mathbf{6}) = \beta_{CT}(\mathbf{9})$ quite reasonable. Since *m*2*m* the crystallographic class of **9**, $b_{eff}(\mathbf{9}) = \sin^2(\phi)\cos(\theta)\sin^2(\theta)\beta_{CT}$, with θ (0.7°) and ϕ (66.2°) the angles intercepted by the ^{3}MLCT* axis on *b* and *c*, respectively. Since the calculated $b_{eff}(\mathbf{9})$ is $0.001\beta_{CT}(\mathbf{9})$, the b_{eff}(**6**)/b_{eff}(**9**) ratio is inadequate to mimic the experimental trend (Table 6). We thus have further evidence that a CT contribution different from the ^{3}MLCT* one must be involved. The experimental trend SHG(**6**) < SHG(**9**) (Table 6) is actually consistent with that of the halides' polarizability (Cl < Br), thus suggesting that X-based orbitals should contribute. This latter suggestion is confirmed by the NLO response of $[CuBr(2,4,6\text{-trimethylquinoline})]_n$ (**8**) and $[CuI(2,4,6\text{-trimethylquinoline})]_n$ (**10**), whose chains are differentiated by the halides: the experimental trend SHG(**8**) < SHG(**10**) (Table 6) does follow that of the halides polarizability (Br < I).

According to the crystallographic class of **8** (*m*2*m*), θ and ϕ (defined as for **9**) have values of 13.9° and 65.5°, respectively. With 2*mm* the point symmetry of **10**, $b_{eff}(\mathbf{10}) = \sin^2(\phi)\cos(\theta)\sin^2(\theta)\beta_{CT}(\mathbf{10})$, with θ (20.6°) and ϕ (0°) the angles intercepted by the ^{3}MLCT* axis on *a* and *b*, respectively. Taking the reasonable assumption that $\beta_{CT}(\mathbf{8}) = \beta_{CT}(\mathbf{10})$, the calculated b_{eff}(**10**)/b_{eff}(**8**) ratio is 0, rather different from the experimental value [SHG(**10**)/SHG(**8**) = 2, Table 6], thus producing further evidence of the inadequacy of taking into account the ^{3}MLCT* process.

With respect to known spectroscopic studies,[6] the emissive behavior of **5**−**10**, alone, does not consent a well-founded statement on the charge-transfer electronic transitions involved in the NLO response. A certain sensitivity of λ_{max}^{em} to the nature of the halide would suggest participation of halide-based orbitals to the major charge-transfer process, while intermetal distances invariably greater than the sum of the van der Waals radii allow us to exclude a $d_{Cu} \rightarrow (s,p)_{Cu}$ contribution from Cu-delocalized orbitals.[6] Moreover,

(27) Ryn, C. K.; Vitale, M.; Ford, P. C. *Inorg. Chem.* **1993**, *32*, 869.
(28) Vitale, M.; Ryn, C. K.; Palke, W. E.; Ford, P. C. *Inorg. Chem.* **1994**, *33*, 561.

the inadequacy of the involvement of a ^{3}MLCT* transition alone emerges from the investigation of the NLO responses via the Zyss model.[25] ^{3}XLCT*'s thus appear as having a significant role in the investigated SHGs. This latter assumption is confirmed by the SHG efficiencies of compounds having the same structural motifs and organic ligands but differing for the halides.

Conclusions

We have not only synthesized and structurally characterized two novel chain and stair copper(I) compounds (among which there is a rare example of the $[CuX(L)_2]_n$ chain motif) showing largely different second-order NLO responses but we have also underlined for the first time that Cu(I) polymeric inorganic−organic materials with pseudoaromatic η^1-nitrogen donor ligands may display second-order NLO activities, as in the case of **4b**. The strength of such activities, similarly to their solid-state luminescent emissions,[5,6] is retraceable to both the bridging halide and the structure of the polymeric framework. Comparison between experimental and calculated SHG efficiencies for a few compounds whose asymmetric units differ either for the η^1-nitrogen donor ligand or for the halide reveals that in no case can a ^{3}MLCT* process alone reproduce the experimental trend of their NLO responses in a satisfactory way. In addition, in all the analyzed chain and stair structures, the intermetal distances are greater than the sum of the van der Waals radii, thus excluding any contribution from Cu-delocalized orbitals to the charge-transfer process, as occurs at variance in $[CuX(L)]_4$ clusters.[6] Accordingly, we have evidence of a significant role for a ^{3}XLCT process.

In addition, we have noticed a clear dependence of the NLO response on the structural motifs, chains showing larger NLO efficiencies than stairs. The major role of the structural arrangement is shown by the larger NLO efficiencies of chains bearing 2,4,6-trimethylpyridine with respect to those with the more π-delocalized 2-methylquinoline. Despite the lower π_L* level of the latter, surely involved in the charge-transfer processes (either ^{3}XLCT or ^{3}MLCT) controlling the NLO response, SHG efficiencies are greater in the former case. Actually, the Zyss model considers the *spatial* orientation of the dipoles, i.e., just their through-space interactions. However, the influence of the halides on the SHGs of the title compounds supports a more complex picture, suggesting that not just through-space but even through-bond interactions are at work: the discrepancy in the NLO performances of chains and stairs could thus be partially explained by considering that the two structural motifs allow different dipole−dipole through-bond interactions.

Acknowledgment. This work was supported by the Ministero dell'Istruzione, dell'Università e della Ricerca and by the Consiglio Nazionale delle Ricerche. We thank Dr. Steve Massick (University of California, Santa Barbara) for help with emission spectroscopy of **4b** and Dr. Vojislav Srdanov (University of California, Santa Barbara) for preliminary help with Kurtz−Perry measurements.

Supporting Information Available: A crystallographic CIF file for **4a** and **4b.** This material is available free of charge via the Internet at http://pubs.acs.org.

CM020640W